technologies

MDPI

Communication

Research on Outdoor Mobile Music Speaker Battery Management Algorithm Based on Dynamic Redundancy

Xiaofei Yu [1], Yanke Li [2], Xiaonan Li [1], Licheng Wang [3] and Kai Wang [1,*]

1 Conservatory of Music, Qingdao University, Qingdao 266000, China
2 School of Electrical Engineering, Weihai Innovation Research Institute, Qingdao University, Qingdao 266000, China
3 School of Information Engineering, Zhejiang University of Technology, Hangzhou 310014, China
* Correspondence: wangkai@qdu.edu.cn or wkwj888@163.com; Tel.: +86-158-6306-0145; Fax: +86-532-8595-1980

Abstract: In terms of the battery management system of a mobile music speaker, reliability optimization has always been an important topic. This paper proposes a new dynamic redundant battery management algorithm based on the existing fault-tolerant structure of a lithium battery pack. The internal configuration is adjusted according to the SOC of each battery, and the power supply battery is dynamically allocated. This paper selects four batteries to experiment on with two different algorithms. The simulation results show that compared with the traditional battery management algorithm, the dynamic redundant battery management algorithm extends the battery pack working time by 18.75%, and the energy utilization rate of B_1 and B_4 increases by 96.0% and 99.8%, respectively. This proves that the dynamic redundant battery management algorithm can effectively extend battery working time and improve energy utilization.

Keywords: dynamic redundancy; music speaker battery; state of charge; fault time; passive redundancy

check for updates

Citation: Yu, X.; Li, Y.; Li, X.; Wang, L.; Wang, K. Research on Outdoor Mobile Music Speaker Battery Management Algorithm Based on Dynamic Redundancy. *Technologies* **2023**, *11*, 60. https://doi.org/10.3390/technologies11020060

Received: 2 February 2023
Revised: 23 March 2023
Accepted: 4 April 2023
Published: 18 April 2023

1. Introduction

With the gradual development of video and audio technology in the 21st century, the development of portable audio source products is diversified [1–3]. For different use environments and users, there are many types of audio source products, such as split type, combined type, desktop type, portable type and outdoor type. Mobile music speakers have become a hot product in recent years. Mobile music speakers are outdoor speakers that can be carried at any time. In a small range, such as classrooms or bedrooms at home, mobile music speakers are convenient as they can play music at any time. In the outdoor environment, outdoor activities often require speaker equipment support, so mobile music speakers are suitable for use in outdoor collective activities, such as teaching, group meetings, shopping mall broadcasting, dance practice and morning exercise audio. In these cases, a mobile music speaker is a good choice. However, though they are convenient and lightweight, mobile music speaker batteries have a short life, are slow to charge and have other problems. Thus, mobile music speaker battery research is a hot issue today. Most mobile music speakers in China use lithium-ion batteries [4–7]. However, with the increasing demand for energy and the increasingly serious environmental pollution caused by traditional energy in the 21st century, new renewable energy sources such as nanogenerators have emerged [8–11]. Further, new energy batteries have flourished in the era of energy conservation and emission reduction [12,13]. In recent years, research on new energy batteries has continued to strengthen, the energy density of batteries has continued to increase [14–18] and the production cost has dropped significantly. In particular, the emergence of lithium-ion batteries has become a hot spot for new energy batteries [19–22]. How to improve the performance of battery packs and reduce the use cost are the research focus of new energy batteries [23–25]. Figure 1 shows the advantages and problems of mobile music speakers.

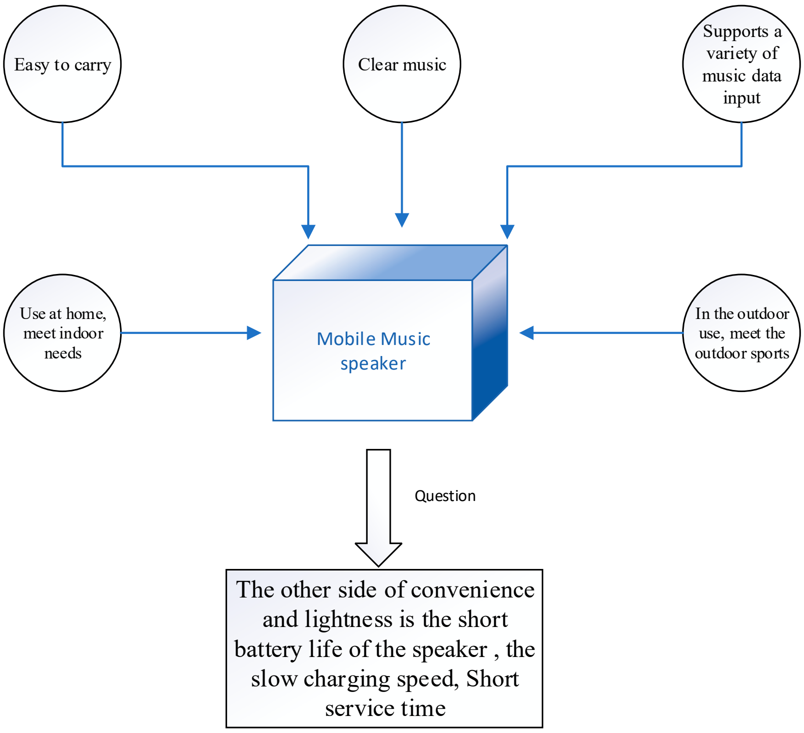

Figure 1. The advantages and problems of mobile music speakers.

In the study of battery pack management systems for mobile music speakers, most researchers improved the service life of the battery pack by studying the inconsistency in batteries [26–30]. This paper proposes a new dynamic redundant battery management algorithm based on the existing fault-tolerant structure of a lithium battery pack, adjusts redundant batteries by identifying the SOC of each battery, minimizes the impact of a single battery failure and improves the overall reliability of the battery pack. Compared with the traditional redundant battery management system, the energy utilization rate of the redundant battery is greatly improved, and the working time of the battery pack is extended, which effectively slows down the aging speed of the battery pack caused by excessive discharge of a single battery. However, the battery management algorithm based on dynamic redundancy uses more batteries, which has a high cost and complex internal circuits that need to be improved.

2. Model Building

The architecture of the battery pack is closely related to the reliability of the entire battery system [31,32]. In order to improve the reliability, one can further extend the working time of the battery by adding redundant units and switches to select active units. The main electrical characteristic of the battery is the maximum storage capacity Q_0. The physical characteristics of the battery are usually characterized by state of charge (SOC) [33–37]. SOC describes the battery's charge $Q(t)$ at time t in the form of a percentage. During calculation, SOC data are equal to the charge quantity $Q(t)$ of the battery at time t divided by the maximum storage capacity Q_0, and its expression is as follows:

$$SOC = \frac{Q(t)}{Q_0} \times 100\% \tag{1}$$

A single battery can only provide nominal current at a preset voltage [38–40]. In order to meet the requirements of power equipment, power storage systems usually use series to increase voltage and parallel to increase current. For example, for two parallel connections of four batteries in series, the instantaneous failure rate of a battery failure is denoted as λ and the overall failure rate is 8λ, resulting in the reliability of the power storage system being greatly reduced. Therefore, it is necessary to use redundant batteries to improve battery reliability. The relationship between reliability $R(t)$ and instantaneous failure rate λ is as follows:

$$R(t) = e^{-\lambda_{cell} \cdot t} \tag{2}$$

The expression of MTTF, the average battery failure time, is:

$$MTTF_{cell} = \int_{t=0}^{+\infty} R(t) \cdot d_t = \frac{1}{\lambda_{cell}} \tag{3}$$

Currently, there are two common fault-tolerant structures in batteries [41–43]: series-parallel fault-tolerant structure (SP) and parallel-series fault-tolerant structure (PS). This paper focuses on the study of the PS structure. In the case of unit failure in the PS structure, the exchange between the basic unit and the redundant unit is enabled by the switch, and the reliability of the battery pack can be improved by adding redundant columns. Due to the parallel structure, the faulty battery can be isolated only by a series switch, and the nominal power of the battery pack is usually guaranteed by adding redundant columns. The PS structure of the battery pack in series is shown in Figure 2.

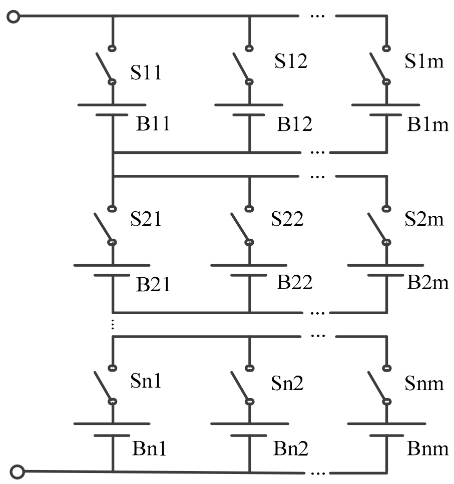

Figure 2. Battery pack parallel-series fault-tolerant structure.

The reliability expression of the PS structure battery is as follows:

$$R_{PS}(t) = e^{-n(m-1)\lambda_{cell}t}(1 + \lambda_{cell}t)^{n(m-1)} \tag{4}$$

The expression MTTF of the mean failure time of the PS structure battery is:

$$MTTF_{PS} = \sum_{k=0}^{n\cdot(m-1)} \binom{n \cdot (m-1)}{k} \frac{1}{n \cdot (m-1)^k \cdot \lambda_{cell}} \tag{5}$$

To demonstrate the operation of the algorithm, power is provided by a set of parallel batteries, one of which is an additional redundant cell. The battery redundancy module, as shown in Figure 3, represents a row in the battery pack architecture, which is capable of providing three-times the power of a single cell.

Among them, B_1, B_2 and B_3 are the main power supply battery, B_4 is the redundant battery, R is the load and each battery is connected with a diode. The main circuit includes four lithium-ion batteries, four relay switches, four diodes and a load. The four batteries are connected in parallel to simulate the actual working state of the battery pack.

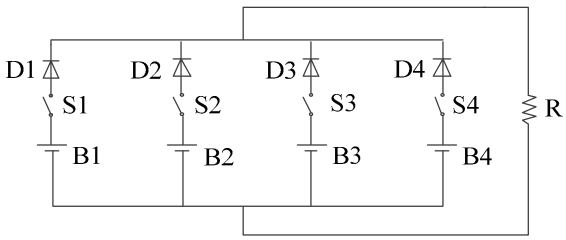

Figure 3. Battery redundancy module.

3. Control Strategy

To ensure that the proposed architecture can meet the power requirements of the external load, three batteries are required to supply external power at any one time. Then, one must fully charge the four batteries and set (SOC) = 1(t = 0). Because the internal resistance and discharge depth of each battery are different, battery strings may be inconsistent during external power supply. Assume that the SOC of each battery drops by 30%, 25%, 20% and 15%, respectively, during each discharge cycle. During each cycle, the SOC of the battery is recorded.

When the traditional redundant battery management system detects that the battery voltage of the working group is lower than the limit value, the redundant battery is started to replace the battery to improve the battery life and anti-interference ability [44,45]. As shown in Table 1, after the 3.3 discharge cycle, the SOC of $B_1 = 0$. It is then isolated and replaced with B_4 redundant batteries. When the SOC of B_2 is 0, the battery string cannot meet the requirement of a triple power supply current. Therefore, the battery string stops supplying power at the fourth discharge cycle.

Table 1. Traditional redundant battery management algorithm discharge process.

				SOC/%
Period of Discharge	**B_1**	**B_2**	**B_3**	**B_4**
0	100	100	100	100
1	70	75	80	100
2	40	50	60	100
3	10	25	40	100
3.3	0	17	33	100
4	0	0	20	85

On this basis, a battery management algorithm based on dynamic redundancy is proposed, as shown in Table 2. Each battery is then charged, with B_1, B_2 and B_3 powered first. After one discharge period, B_1 has the lowest battery capacity and is isolated as a redundant battery. B_2, B_3 and B_4 start to supply the external power. At the end of the second discharge cycle, B_2 has the lowest power, and it is isolated as a new redundant battery, and B_1, B_3 and B_4 supply power. After the end of the fifth discharge cycle, the quantity of B_2 is zero, and only three batteries are left to supply power. After the end of the 5.3 discharge cycle, the quantity of B_1 is zero. At this time, the battery pack cannot meet the requirement of the triple power supply current and the power supply stops. Through the battery management algorithm based on dynamic redundancy, the battery pack discharge period is extended to 5.3. Compared with the traditional redundant battery management algorithm, the working time is significantly extended. Meanwhile, the remaining power of each battery is lower, which improves the utilization rate of energy.

Table 2. Dynamic redundant battery management algorithm discharge process.

					SOC/%
Period of Discharge	B_1	B_2	B_3	B_4	Supply Current
0	100	100	100	100	B_1 B_2 B_3
1	70	75	80	100	B_2 B_3 B_4
2	70	50	60	85	B_1 B_3 B_4
3	40	50	40	70	B_1 B_2 B_4
4	10	25	40	55	B_2 B_3 B_4
5	10	0	20	40	B_1 B_3 B_4
5.3	0	0	13	35	

An algorithm flowchart is shown in Figure 4.

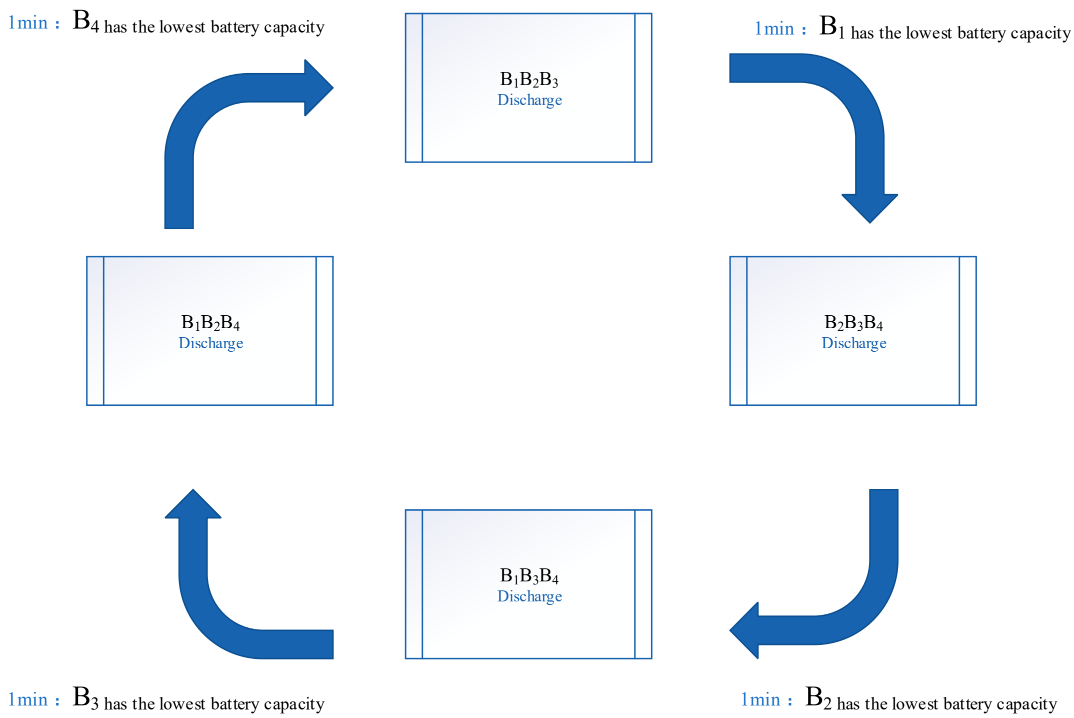

Figure 4. Algorithm flow chart.

4. Simulation Results and Analysis

MATLAB was used for simulation experiments. The initial capacity of the battery was set to 200 mAh, the rated voltage was set to 4 V and the load resistance was set to 5 Ω. In this paper, four batteries were simulated to provide electric energy for power equipment. Due to different production and manufacturing factors and equivalent resistance inside batteries, the initial SOC of the four batteries was selected to be 100%, 90%, 80% and 100%, respectively, in order to make the experiment more universal. When the early discharge of a battery ends, the failed battery is replaced by redundant batteries to ensure the normal operation of the entire battery pack.

The following is the construction of the simulation diagram, divided into main circuit and control circuit, using MATLAB FUNCTION in MATLAB to replace the MCU simulation. First, the main circuit is built. The main circuit consists of four lithium-ion batteries, four relay switches, four diodes, four resistors and one load. The selected battery model can set initial voltage, initial capacity, voltage at full charge and initial SOC. This will facilitate the test of this project. The selected relay switch can be set with internal resistance. In order to simulate the operation under ideal conditions, the internal resistance of the relay is set very small, which can be basically ignored. The same diode can also be set as internal resistance. In order to simulate the operation under ideal conditions, this simulation will set the internal resistance of the diode as very small to facilitate subsequent test analysis. The load selected for the main circuit is also adjustable, so as to facilitate waveform analysis. This is the complete device introduction of the main circuit, and the main circuit is shown in Figure 5 below.

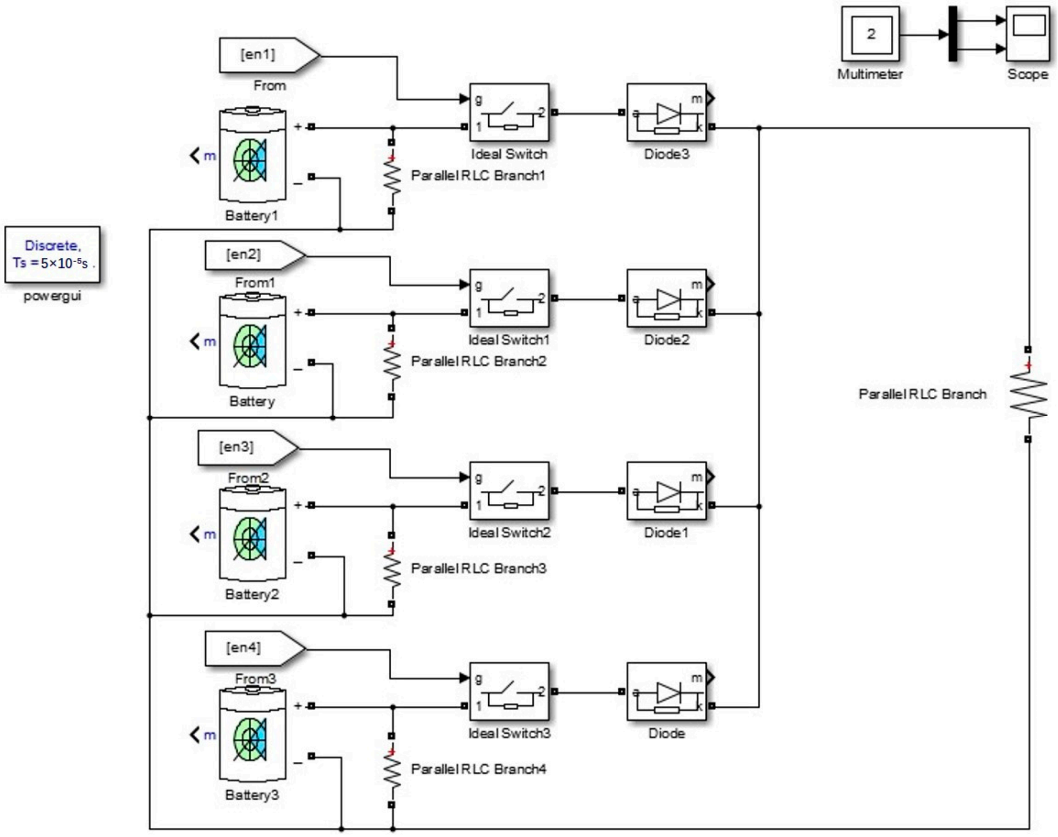

Figure 5. Main circuit of algorithm.

The control circuit is shown in Figure 6. Firstly, MATLAB FUNCTION is used to simulate the single chip microcomputer to realize the algorithm research. This function can realize the same function as the single chip microcomputer. Then, the control circuit is built. The specific idea is as follows: when the high level of the pulse generator is produced, the timing will start when only the delayed input also enters a high level. Knowing that the next pulse is high, the delayed pulse will arrive along the rising edge, thus realizing the function of the cycle and having a time period that can be adjusted. Then, MATLAB programming is utilized for each cycle of the collected voltage analysis. Selecting the battery with the lowest voltage as the standby battery, power is supplied to the other three batteries. After one cycle, MATLAB collects the voltage again and then selects the lowest voltage from the four batteries as the new standby battery. This cycle equalizes the battery pack.

The discharge process of traditional redundant battery management algorithms is as follows: B_1, B_2 and B_3 are discharged first, and B_4 is used as the redundant battery. B_3 is the first battery whose SOC decreases to 0. When the SOC of B_3 decreases to 0, it is replaced by B_4, B_1, B_2 and B_4 to continue the work.

The discharge process of the battery management algorithm based on dynamic redundancy is shown in Figure 7. During the working process of the battery pack, the sampling time t = 1 min is set, and the SOC of the four batteries is compared every 1 min, so as to ensure that the battery with the highest SOC always supplies power to the outside in each time period. As can be seen from the figure, at the beginning of discharge, the SOC of the four batteries is compared, and B_3 is the least redundant battery, while B_1, B_2 and B_4 work. At the 80th minute, B_2 with the smallest SOC is selected as the redundant battery, and B_1, B_3 and B_4 continue to work. At the next sampling time, the same operation is carried out, and the cycle is carried out. Compared with the traditional redundant battery discharge method, the operating time of the dynamically redundant battery pack reaches 190 min, which is 18.75% longer.

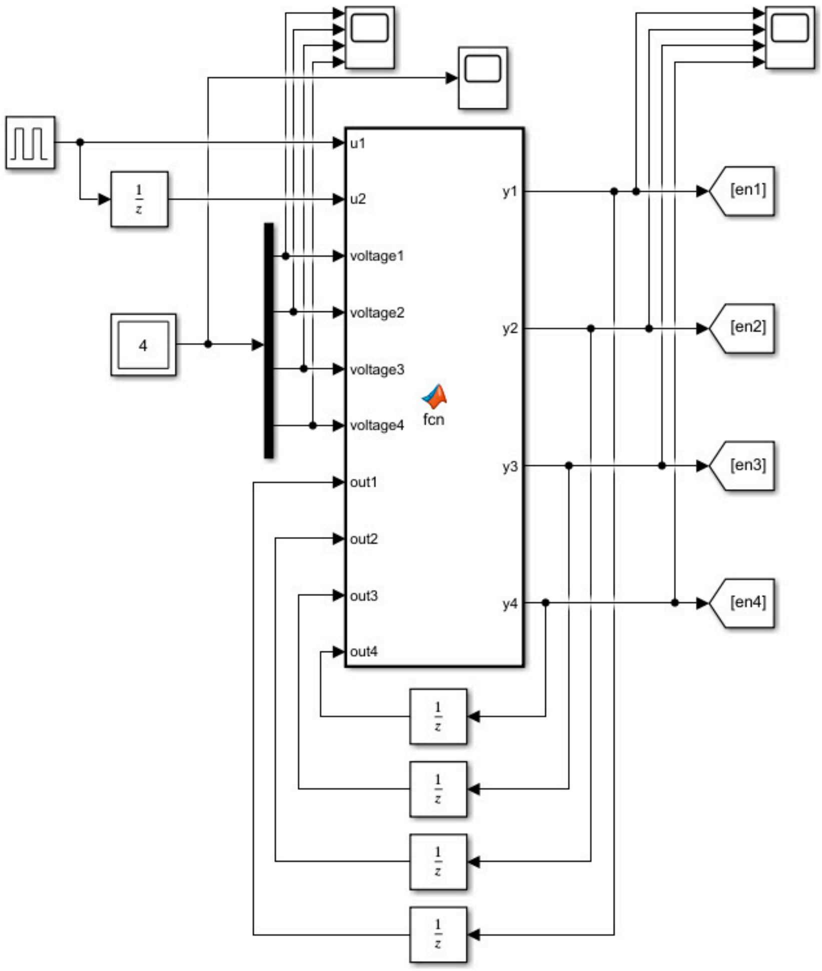

Figure 6. Control circuit of algorithm.

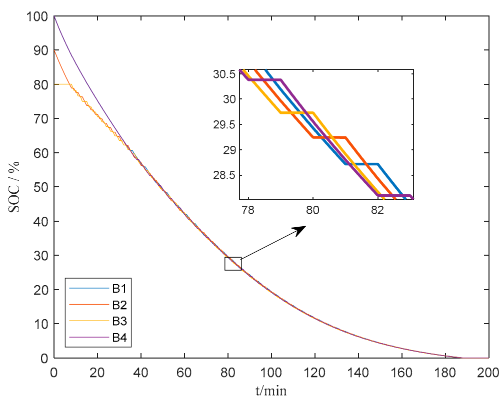

Figure 7. Dynamic redundant battery management algorithm working process diagram.

The simulation circuit is run, and the relay operation process of each battery in series is shown in Figure 8. A large resistance is connected in parallel at both ends of the relay to detect the opening and closing of the relay. The high level represents the closing of the relay, while the low level represents the disconnection of the relay. As can be seen from the figure, in each discharge cycle, three batteries are at a high level and one battery is at a low level to meet the load requirements. The power supply process for the whole battery pack is a process of dynamic selection.

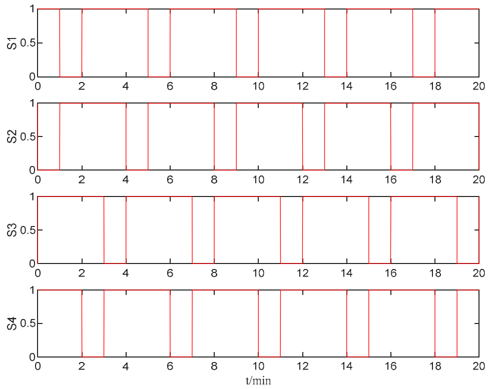

Figure 8. Relay switch action.

The SOC after a single discharge of the traditional redundant battery management algorithm is shown in Table 3. It can be seen that when the traditional redundant battery management algorithm ends the discharge of 160 min, the remaining SOC of B_1 is 2.5%, B_2 and B_3 are reduced to 0 and the remaining SOC of B_4 is 58.1%.

Table 3. Traditional redundant battery management algorithm.

				SOC/%
t/min	**B_1**	**B_2**	**B_3**	**B_4**
0	100.0	90.0	80.0	100.0
30	63.3	55.7	48.4	100.0
60	37.7	31.4	27.1	100.0
100	14.4	11.1	7.7	100.0
130	5.6	4.3	0	100.0
160	2.5	0	0	58.1

The SOC after a single discharge of the battery management algorithm based on dynamic redundancy is shown in Table 4. At the end of 190 min of discharge, the remaining SOC of B_1 is 0.1%, B_2 and B_3 are reduced to 0 and the remaining SOC of B_4 is 0.1%. Compared with the traditional redundant battery management algorithm, the remaining battery power is significantly lower, and the energy utilization rate of B_1 and B_4 is increased by 96.0% and 99.8%, respectively.

Table 4. Dynamic redundant battery management algorithm.

				SOC/%
t/min	**B_1**	**B_2**	**B_3**	**B_4**
0	100.0	90.0	80.0	100.0
30	65.5	64.6	63.8	66.4
60	42.8	42.3	43.0	42.7
100	19.7	20.0	19.9	19.6
130	9.2	8.9	9.0	8.9
160	3.0	2.9	2.9	3.1
190	0.1	0	0	0.1

Although the battery management algorithm based on dynamic redundancy can improve the energy utilization rate of the battery and improve the reliability of the battery pack, the battery management algorithm based on dynamic redundancy needs to be improved due to the high cost and complex internal circuit.

5. Conclusions

In this paper, a battery management algorithm based on dynamic redundancy is proposed for the battery management system of a mobile music speaker. Through dynamic adjustment of redundant batteries under various working conditions, the voltage output can be stable, and the working time of battery packs can be extended. Through MATLAB simulation to verify the algorithm, a single discharge process of the battery pack working time increased from 160 min to 190 min, extended by 18.75%; At the same time, the energy utilization rates of B1 and B4 were increased by 96.0% and 99.8% respectively based on the remaining power of redundant batteries. The results show that the proposed battery management scheme can greatly reduce the impact of single battery failure, improve the reliability of the battery and slow down the aging speed of the battery caused by excessive discharge of a single battery.

Author Contributions: The named authors have substantially contributed to conducting the underlying research and drafting this manuscript. Conceptualization, X.Y.; methodology, X.Y.; software, Y.L.; validation, X.L., L.W.; formal analysis, X.L.; investigation, L.W.; data curation, K.W.; writing—original draft preparation, X.Y.; writing—review and editing, Y.L.; visualization, L.W.; supervision, K.W.; project administration, K.W.; funding acquisition, K.W. All authors have read and agreed to the published version of the manuscript.

Funding: This work was supported by the Shandong University Youth Innovation Team Development Plan (No. 2021RW012), National Social Science Foundation Art Program (20CD173), the Youth Fund of Shandong Province Natural Science Foundation (No. ZR2020QE212), Key Projects of Shandong Province Natural Science Foundation (No. ZR2020KF020), the Guangdong Provincial Key Lab of Green Chemical Product Technology (No. GC 202111), Zhejiang Province Natural Science Foundation (No. LY22E070007) and National Natural Science Foundation of China (No. 52007170).

Informed Consent Statement: Informed consent was obtained from all subjects involved in the study.

Data Availability Statement: The data and materials used to support the findings of this study are available from the corresponding author upon request.

Conflicts of Interest: The authors declare no conflict of interest.

References

1. Cao, Y.; Li, K.; Lu, M. Balancing Method Based on Flyback Converter for Series-Connected Cells. *IEEE Access* **2021**, *9*, 52393–52403. [CrossRef]
2. Che, Y.; Deng, Z.; Tang, X.; Lin, X.; Nie, X.; Hu, X. Lifetime and Aging Degradation Prognostics for Lithium-ion Battery Packs Based on a Cell to Pack Method. *Chin. J. Mech. Eng.* **2022**, *35*, 4. [CrossRef]
3. Jiang, C.; Wang, S.; Wu, B.; Fernandez, C.; Xiong, X.; Coffie-Ken, J. A state-of-charge estimation method of the power lithium-ion battery in complex conditions based on adaptive square root extended Kalman filter. *Energy* **2021**, *219*, 119603. [CrossRef]
4. Yu, X.; Bao, A. Tian Liantao and the Discipline Construction of Chinese Minority Music. *J. Cent. Conserv. Music* **2022**, *169*, 63–72.
5. Yu, X. Research on Contemporary Minority Musicians from the Perspective of Oral History. *Arts Crit.* **2020**, *201*, 84–93.
6. Yu, X. The Oral History Path in the Study of Contemporary Musicians: Significance, Theory, and Method. *Hundred Sch. Arts* **2022**, *38*, 113–119.
7. Yu, X.; Ma, N.; Zheng, L.; Wang, L.; Wang, K. Developments and Applications of Artificial Intelligence in Music Education. *Technologies* **2023**, *11*, 42. [CrossRef]
8. Zhang, M.; Wang, W.; Xia, G.; Wang, L.; Wang, K. Self-Powered Electronic Skin for Remote Human–Machine Synchronization. *ACS Appl. Electron. Mater.* **2023**, *5*, 498–508. [CrossRef]
9. Wang, W.; Yang, D.; Yan, X.; Wang, L.; Hu, H.; Wang, K. Triboelectric nanogenerators: The beginning of blue dream. *Front. Chem. Sci. Eng.* **2023**. [CrossRef]
10. Wang, W.; Yang, D.; Huang, Z.; Hu, H.; Wang, L.; Wang, K. Electrodeless Nanogenerator for Dust Recover. *Energy Technol.* **2022**, *10*, 2200699. [CrossRef]
11. Wang, W.; Pang, J.; Su, J.; Li, F.; Li, Q.; Wang, X.; Wang, J.; Ibarlucea, B.; Liu, X.; Li, Y. Applications of nanogenerators for biomedical engineering and healthcare systems. *InfoMat* **2022**, *4*, e12262. [CrossRef]

12. Kim, J.; Kowal, J. A Method for Detecting the Existence of an Over-Discharged Cell in a Lithium-Ion Battery Pack via Measuring Total Harmonic Distortion. *Batteries* **2022**, *8*, 26. [CrossRef]
13. Ko, H.; Pack, S.; Leung, V.C.M. An Optimal Battery Charging Algorithm in Electric Vehicle-Assisted Battery Swapping Environments. *IEEE Trans. Intell. Transp. Syst.* **2022**, *23*, 3985–3994. [CrossRef]
14. Guo, Y.; Yang, D.; Zhang, Y.; Wang, L.; Wang, K. Online estimation of SOH for lithium-ion battery based on SSA-Elman neural network. *Prot. Control Mod. Power Syst.* **2022**, *7*, 40. [CrossRef]
15. Cui, Z.; Kang, L.; Li, L.; Wang, L.; Wang, K. A combined state-of-charge estimation method for lithium-ion battery using an improved BGRU network and UKF. *Energy* **2022**, *259*, 124933. [CrossRef]
16. Zhang, M.; Wang, K.; Zhou, Y.-T. Online state of charge estimation of lithium-ion cells using particle filter-based hybrid filtering approach. *Complexity* **2020**, *2020*, 8231243. [CrossRef]
17. Zhang, M.; Liu, Y.; Li, D.; Cui, X.; Wang, L.; Li, L.; Wang, K. Electrochemical Impedance Spectroscopy: A New Chapter in the Fast and Accurate Estimation of the State of Health for Lithium-Ion Batteries. *Energies* **2023**, *16*, 1599. [CrossRef]
18. Li, D.; Yang, D.; Li, L.; Wang, L.; Wang, K. Electrochemical Impedance Spectroscopy Based on the State of Health Estimation for Lithium-Ion Batteries. *Energies* **2022**, *15*, 6665. [CrossRef]
19. Lan, T.; Jermsittiparsert, K.; Alrashood, S.T.; Rezaei, M.; Al-Ghussain, L.; Mohamed, M.A. An Advanced Machine Learning Based Energy Management of Renewable Microgrids Considering Hybrid Electric Vehicles' Charging Demand. *Energies* **2021**, *14*, 569. [CrossRef]
20. Li, A.; Yuen, A.C.Y.; Wang, W.; Chen, T.B.Y.; Lai, C.S.; Yang, W.; Wu, W.; Chan, Q.N.; Kook, S.; Yeoh, G.H. Integration of Computational Fluid Dynamics and Artificial Neural Network for Optimization Design of Battery Thermal Management System. *Batteries* **2022**, *8*, 69. [CrossRef]
21. Mallon, K.; Assadian, F. A Study of Control Methodologies for the Trade-Off between Battery Aging and Energy Consumption on Electric Vehicles with Hybrid Energy Storage Systems. *Energies* **2022**, *15*, 600. [CrossRef]
22. Peng, J.; Shi, H.; Wang, S.; Wang, L.; Fernandez, C.; Xiong, X.; Dablu, B.E. A novel equivalent modeling method combined with the splice-electrochemical polarization model and prior generalized inverse least-square parameter identification for UAV lithium-ion batteries. *Energy Sci. Eng.* **2022**, *10*, 3727–3740. [CrossRef]
23. Shu, X.; Li, G.; Zhang, Y.; Shen, S.; Chen, Z.; Liu, Y. Stage of Charge Estimation of Lithium-Ion Battery Packs Based on Improved Cubature Kalman Filter With Long Short-Term Memory Model. *IEEE Trans. Transp. Electrif.* **2021**, *7*, 1271–1284. [CrossRef]
24. Shu, X.; Shen, J.; Li, G.; Zhang, Y.; Chen, Z.; Liu, Y. A Flexible State-of-Health Prediction Scheme for Lithium-Ion Battery Packs With Long Short-Term Memory Network and Transfer Learning. *IEEE Trans. Transp. Electrif.* **2021**, *7*, 2238–2248. [CrossRef]
25. Tang, X.; Gao, F.; Liu, K.; Liu, Q.; Foley, A.M. A Balancing Current Ratio Based State-of-Health Estimation Solution for Lithium-Ion Battery Pack. *IEEE Trans. Ind. Electron.* **2022**, *69*, 8055–8065. [CrossRef]
26. Tran, M.-K.; Cunanan, C.; Panchal, S.; Fraser, R.; Fowler, M. Investigation of Individual Cells Replacement Concept in Lithium-Ion Battery Packs with Analysis on Economic Feasibility and Pack Design Requirements. *Processes* **2021**, *9*, 2263. [CrossRef]
27. Wang, J.; Zhang, S.; Hu, X. A Fault Diagnosis Method for Lithium-Ion Battery Packs Using Improved RBF Neural Network. *Front. Energy Res.* **2021**, *9*, 702139. [CrossRef]
28. Wang, K.; Liu, C.; Sun, J.; Zhao, K.; Wang, L.; Song, J.; Duan, C.; Li, L. State of Charge Estimation of Composite Energy Storage Systems with Supercapacitors and Lithium Batteries. *Complexity* **2021**, *2021*, 8816250. [CrossRef]
29. Wei, Z.; Quan, Z.; Wu, J.; Li, Y.; Pou, J.; Zhong, H. Deep Deterministic Policy Gradient-DRL Enabled Multiphysics-Constrained Fast Charging of Lithium-Ion Battery. *IEEE Trans. Ind. Electron.* **2022**, *69*, 2588–2598. [CrossRef]
30. Yang, R.; Xiong, R.; Shen, W.; Lin, X. Extreme Learning Machine-Based Thermal Model for Lithium-Ion Batteries of Electric Vehicles under External Short Circuit. *Engineering* **2021**, *7*, 395–405. [CrossRef]
31. Wang, L.; Xie, L.; Yang, Y.; Zhang, Y.; Wang, K.; Cheng, S.-J. Distributed Online Voltage Control with Fast PV Power Fluctuations and Imperfect Communication. *IEEE Trans. Smart Grid* **2023**. [CrossRef]
32. Ma, N.; Yang, D.; Riaz, S.; Wang, L.; Wang, K. Aging Mechanism and Models of Supercapacitors: A Review. *Technologies* **2023**, *11*, 38. [CrossRef]
33. Hu, W.; Zhao, S. Remaining useful life prediction of lithium-ion batteries based on wavelet denoising and transformer neural network. *Front. Energy Res.* **2022**, *10*, 969168. [CrossRef]
34. Feng, H.; Yan, H. State of health estimation of large-cycle lithium-ion batteries based on error compensation of autoregressive model. *J. Energy Storage* **2022**, *52*, 104869. [CrossRef]
35. Xu, X.; Sun, X.; Zhao, L.; Li, R.; Tang, W. Research on thermal runaway characteristics of NCM lithium-ion battery under thermal-electrical coupling abuse. *Ionics* **2022**, *28*, 5449–5467. [CrossRef]
36. Hsiang, H.-I.; Chen, W.-Y. Electrochemical Properties and the Adsorption of Lithium Ions in the Brine of Lithium-Ion Sieves Prepared from Spent Lithium Iron Phosphate Batteries. *Sustainability* **2022**, *14*, 16235. [CrossRef]
37. Ouyang, M.; Shen, P. Prediction of Remaining Useful Life of Lithium Batteries Based on WOA-VMD and LSTM. *Energies* **2022**, *15*, 8918. [CrossRef]
38. Zhang, M.; Yang, D.; Du, J.; Sun, H.; Li, L.; Wang, L.; Wang, K. A Review of SOH Prediction of Li-Ion Batteries Based on Data-Driven Algorithms. *Energies* **2023**, *16*, 3167. [CrossRef]
39. Lv, S.; Wang, X.; Lu, W.; Zhang, J.; Ni, H. The Influence of Temperature on the Capacity of Lithium Ion Batteries with Different Anodes. *Energies* **2022**, *15*, 60. [CrossRef]

40. Liu, Q.; Zhu, Q.; Zhu, W.; Yi, X.; Han, X. Thermal Runaway Characteristics of 18650 NCM Lithium-ion Batteries under the Different Initial Pressures. *Electrochemistry* **2022**, *90*, 087004. [CrossRef]
41. Liu, J.; Duan, Q.; Qi, K.; Liu, Y.; Sun, J.; Wang, Z.; Wang, Q. Capacity fading mechanisms and state of health prediction of commercial lithium-ion battery in total lifespan. *J. Energy Storage* **2022**, *46*, 103910. [CrossRef]
42. Chen, D.; Zheng, X.; Chen, C.; Zhao, W. Remaining useful life prediction of the lithium-ion battery based on CNN-LSTM fusion model and grey relational analysis. *Electron. Res. Arch.* **2022**, *31*, 633–655. [CrossRef]
43. Wang, H.; Yu, K.; Mao, L.; He, Q.; Wu, Q.; Li, Z. Evaluation of Lithium-Ion Battery Pack Capacity Consistency Using One-Dimensional Magnetic Field Scanning. *IEEE Trans. Instrum. Meas.* **2022**, *71*, 3507610. [CrossRef]
44. Zhang, C.-Y.; Wang, S.-L.; Yu, C.-M.; Xie, Y.-X.; Fernandez, C. Improved Particle Swarm Optimization-Extreme Learning Machine Modeling Strategies for the Accurate Lithium-ion Battery State of Health Estimation and High-adaptability Remaining Useful Life Prediction. *J. Electrochem. Soc.* **2022**, *169*, 080520. [CrossRef]
45. Yuan, B.; Zhang, B.; Yuan, X.; Wang, J.; Chen, L.; Bai, L.; Luo, S. Study on the Relationship Between Open-Circuit Voltage, Time Constant And Polarization Resistance of Lithium-Ion Batteries. *J. Electrochem. Soc.* **2022**, *169*, 060513. [CrossRef]